Science
AAAS

Cleavage of NIK by the API2-MALT1 Fusion Oncoprotein Leads to Noncanonical NF- κB Activation

Shaun Rosebeck, *et al.*

Science **331**, 468 (2011);
DOI: 10.1126/science.1198946

Cleavage of NIK by the API2-MALT1 Fusion Oncoprotein Leads to Noncanonical NF-κB Activation

Shaun Rosebeck,[1]‡ Lisa Madden,[1]*‡ Xiaohong Jin,[2] Shufang Gu,[1] Ingrid J. Apel,[2] Alex Appert,[3] Rifat A. Hamoudi,[3] Heidi Noels,[4,5]† Xavier Sagaert,[6] Peter Van Loo,[4,5] Mathijs Baens,[4,5] Ming-Qing Du,[3] Peter C. Lucas,[2]§ Linda M. McAllister-Lucas[1]§

Proper regulation of nuclear factor κB (NF-κB) transcriptional activity is required for normal lymphocyte function, and deregulated NF-κB signaling can facilitate lymphomagenesis. We demonstrate that the API2-MALT1 fusion oncoprotein created by the recurrent t(11;18)(q21;q21) in mucosa-associated lymphoid tissue (MALT) lymphoma induces proteolytic cleavage of NF-κB–inducing kinase (NIK) at arginine 325. NIK cleavage requires the concerted actions of both fusion partners and generates a C-terminal NIK fragment that retains kinase activity and is resistant to proteasomal degradation. The resulting deregulated NIK activity is associated with constitutive noncanonical NF-κB signaling, enhanced B cell adhesion, and apoptosis resistance. Our study reveals the gain-of-function proteolytic activity of a fusion oncoprotein and highlights the importance of the noncanonical NF-κB pathway in B lymphoproliferative disease.

Mucosa-associated lymphoid tissue (MALT) lymphoma, the most common extranodal B cell tumor, accounts for 8% of non-Hodgkin's lymphomas (*1*). The API2-MALT1 fusion oncoprotein present in t(11;18)-positive MALT lymphomas is composed of the N terminus of API2 [also termed cellular inhibitor of apoptosis 2 (cIAP2)] linked to the C terminus of MALT1 (*1*). Wild-type MALT1 mediates antigen-induced nuclear factor κB (NF-κB) stimulation, which leads to lymphocyte survival and proliferation (*2*). MALT1 activates canonical NF-κB signaling after autooligomerization induced by upstream

[1]Department of Pediatrics and Communicable Diseases, University of Michigan, 1150 West Medical Center Drive, Ann Arbor, MI, 48109, USA. [2]Department of Pathology, University of Michigan, 1150 West Medical Center Drive, Ann Arbor, MI, 48109, USA. [3]Division of Molecular Histopathology, Department of Pathology, University of Cambridge, Laboratory Block, Addenbrooke's Hospital, Hills Road, Cambridge CB2 0QQ, UK. [4]Human Genome Laboratory, Molecular Genetics, Center for Human Genetics, Catholic University Leuven, B-3000 Leuven, Belgium. [5]Human Genome Laboratory, Department of Molecular and Developmental Genetics, Flanders Institute for Biotechnology (VIB), B-3000 Leuven, Belgium. [6]Section of Morphology and Molecular Pathology, Department of Pathology, Catholic University Leuven, B-3000 Leuven, Belgium.

*Present address: Department of Pediatrics, Washington University School of Medicine, 660 South Euclid Avenue, St. Louis, MO 63110, USA.

†Present address: Institute for Molecular Cardiovascular Research, RWTH Aachen University, 52074 Aachen, Germany.

‡These authors contributed equally to the work.

§To whom correspondence should be addressed. E-mail: plucas@umich.edu (P.C.L.); lindaluc@umich.edu (L.M.M-L.)

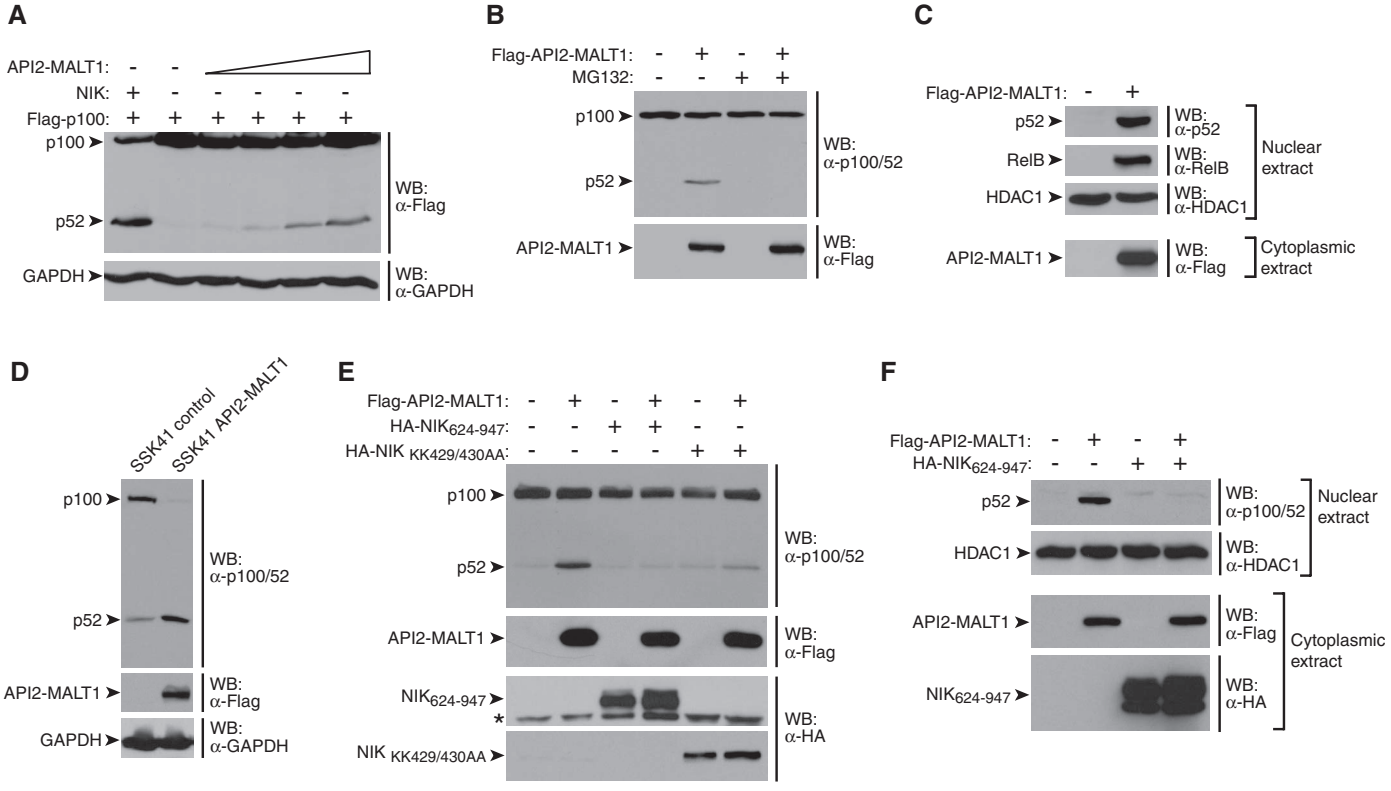

Fig. 1. API2-MALT1 induces noncanonical NF-κB signaling through NIK. (**A** and **B**) HEK293T cells were transfected as indicated, and p100 processing to p52 was assessed by Western blot (WB) with an antibody against Flag (α-Flag) (A) or α-p100/52 (to detect endogenous p100/52) (B). Where indicated, cells were treated with proteasome inhibitor, MG132. (**C**) After transfection of HEK293T cells, nuclear extracts were prepared and analyzed for p52 and RelB by WB. (**D**) p100 processing in lysates from control SSK41 cells or SSK41 cells stably expressing API2-MALT1 was analyzed by WB. (**E** and **F**) HEK293T cells were transfected with API2-MALT1 in the absence or presence of NIK mutants. Endogenous p100 processing was analyzed by WB (E), or nuclear extracts were analyzed for the presence of p52 (F). *Nonspecific band. HDAC1, histone deacetylase 1 (loading control for nuclear extract). Data are representative of at least three separate experiments.

factors CARMA1 and Bcl10 (*3*, *4*). It is thought that because the API2 moiety mediates autooligomerization, API2-MALT1 can stimulate NF-κB independent of upstream signals (*5*, *6*). This may explain why t(11;18)-positive MALT lymphomas are not dependent on antigenic stimulation for progression, whereas t(11;18)-negative tumors require ongoing chronic inflammation for survival. The phenomenon is best exemplified by gastric MALT lymphomas, the majority of which arise in the setting of chronic *Helicobacter pylori* gastritis and are cured by eradication of *H. pylori* with antibiotics. In contrast, t(11;18)-positive gastric tumors are resistant to this treatment and are associated with advanced-stage disease (*1*).

We discovered that besides activating canonical NF-κB, expression of API2-MALT1 in human embryonic kidney 293T (HEK293T) or the human B lymphoma (SSK41) cells induced proteasome-dependent processing of the NF-κB precursor, p100, to its mature form, p52, and stimulated nuclear translocation of p52/RelB (Fig. 1, A to D, and fig. S1) (*7*). These findings indicate that API2-MALT1 activates the "noncanonical" NF-κB pathway, which requires NF-κB–inducing kinase (NIK)–dependent phosphorylation and activation of inhibitor of NF-κB (IκB) kinase-α (IKKα). This, in turn, triggers proteasome-mediated partial degradation of p100 to p52 and generation of transcriptionally active p52/RelB NF-κB dimers (*8*). Consistent with this notion, dominant-negative NIK mutants (*9*, *10*) blocked API2-MALT1–dependent p100 processing and p52 nuclear translocation (Fig. 1, E and F).

cIAP1 and cIAP2 (API2) associate with NIK and promote NIK degradation via RING domain ubiquitin ligase activity (*11*–*13*). We hypothesized that API2-MALT1, which lacks the cIAP2 RING domain, stimulates noncanonical signaling through competitive inhibition of cIAP-mediated NIK degradation. In testing this, we discovered that expression of API2-MALT1 instead induced proteolytic cleavage of NIK, generating ~37-kD N-terminal and ~70-kD C-terminal NIK fragments (Fig. 2, A and B, and fig. S2).

API2-MALT1 fusion transcripts invariably contain three intact baculoviral IAP repeat (BIR) domains from API2 and an intact "caspaselike" domain from MALT1, which suggests that these domains are critical for lymphomagenesis (*1*). The caspaselike domain of wild-type MALT1 has proteolytic activity, and Bcl10 and the NF-κB inhibitor, A20, are the only known substrates (*14*, *15*). We therefore investigated whether the caspaselike domain within API2-MALT1 is also able to cleave NIK. Deletion mutants of API2-MALT1 lacking portions of the caspaselike domain and API2-MALT1-C678A (*16*), in which the catalytic cysteine within the MALT1 proteolytic domain is replaced with alanine, were unable to induce NIK cleavage (Fig. 2C and fig. S3, A to C). Furthermore, treatment with z-Val-Arg-Pro-Arg-fluoromethylketone (z-VRPR-fmk), a MALT1 protease inhibitor (*15*), blocked API2-MALT1–induced NIK cleavage, whereas z-IETD-fmk, a caspase-8 inhibitor, had no effect (fig. S3, D and E). Finally, an in vitro cleavage reaction using purified recombinant proteins showed that NIK is a direct substrate of the MALT1 protease domain (Fig. 2D and fig. S4).

Cellular expression of the MALT1 moiety alone was unable to induce NIK cleavage, which suggests that the API2 moiety also contributes in some way (Fig. 2E). Indeed, analyses revealed that NIK physically associates with API2-MALT1 via the API2 moiety (Fig. 2F) and that the region within the API2 moiety that mediates autooligomerization of API2-MALT1 (amino acids 49 to 98) (*5*) is required for efficient API2-MALT1–dependent NIK cleavage and p100 processing (fig. S5). The collaborative relationship of the

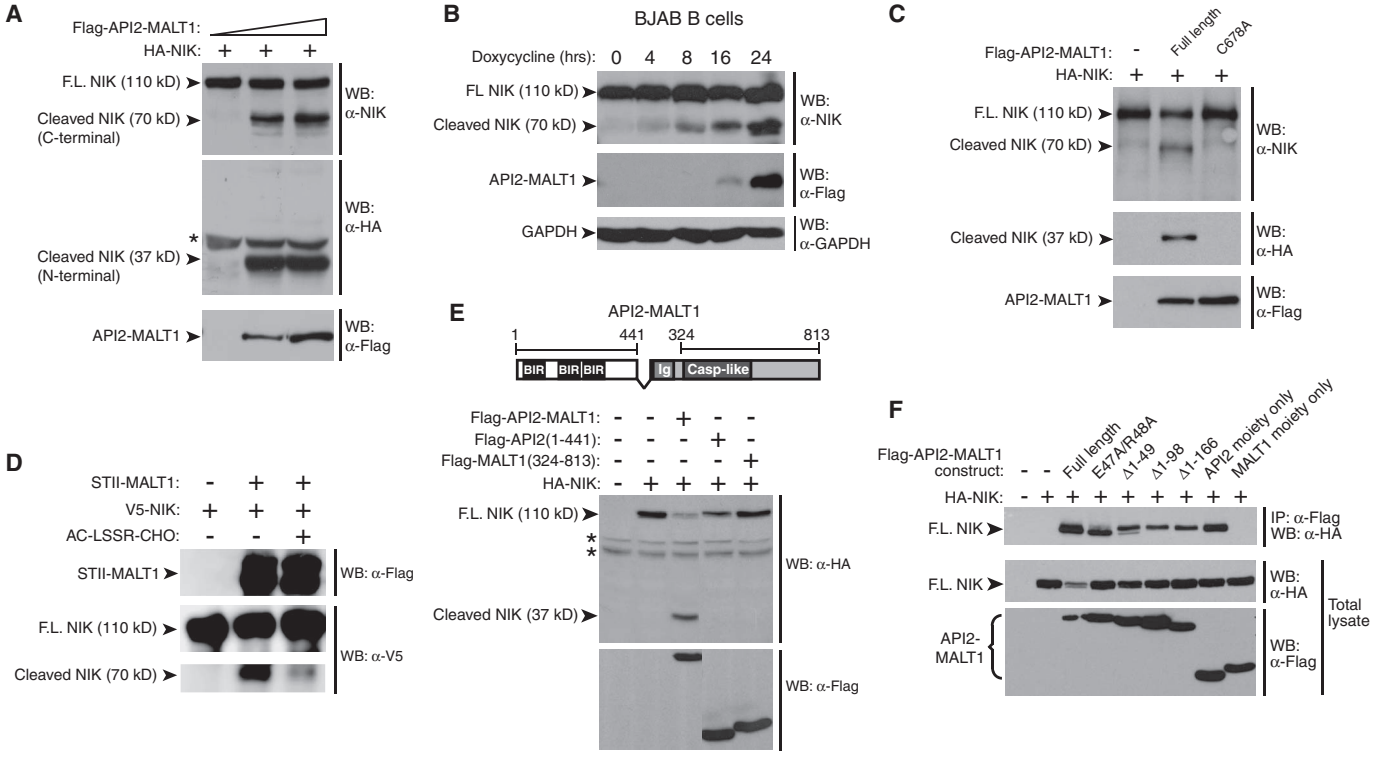

Fig. 2. API2-MALT1 induces NIK cleavage, a phenomenon requiring both the API2 moiety and MALT1 protease activity. (**A**) HEK293T cells were transfected as indicated, and NIK cleavage fragments were detected by WB. (**B**) BJAB cells expressing API2-MALT1 from a tetracycline-inducible promoter were treated with doxycycline. WB with an antibody raised against a C-terminal NIK sequence revealed time-dependent generation of an endogenous 70-kD NIK cleavage fragment. To enhance detection of full-length (FL) NIK, cells were incubated with 25 μM MG132. (**C**) HEK293T cells were transfected as indicated, and the presence of the N-terminal 37-kD and the C-terminal 70-kD NIK cleavage fragments was analyzed by WB. (**D**) Recombinant purified NIK-V5-bioC and StrepII-Flag–tagged MALT1 were incubated in kosmotropic salt buffer for 6 hours at 37°C, with or without 100 μM MALT1 protease inhibitor Ac-LSSR-CHO, and analyzed by WB. (**E**) HEK293T cells were transfected as indicated, and the 37-kD NIK cleavage fragment was detected by WB. (**F**) HEK293T cells were transfected, and immunoprecipitations were carried out using α-Flag–agarose. For a detailed description of API2-MALT1 mutants, see the legend to fig. S5. *Nonspecific band. Data are representative of at least three separate experiments.

API2 and MALT1 moieties in achieving NIK cleavage was further underscored in several different contexts. First, unlike API2-MALT1, induced expression of wild-type MALT1 in BJAB B cells did not result in NIK cleavage (fig. S6A). Second, NIK cleavage was not observed in SSK41 B cells, which are characterized by *MALT1* gene amplification, overexpression of MALT1, and constitutive MALT1 protease activity (*14*, *17*, *18*). In contrast to A20, NIK was cleaved only if SSK41 cells were engineered to express API2-MALT1 (fig. S6B). Third, coexpression of wild-type MALT1 with Bcl10, which triggers MALT1 oligomerization and activation (*3*), did lead to cleavage of A20 but not of NIK (fig. S6, C and D). Fourth, ligand-induced B cell receptor stimulation, which similarly activates the MALT1 protease (*14*), did not trigger NIK cleavage (fig. S6E). Furthermore, although MALT1 oligomerization and activation require Bcl10 (*3*), API2-MALT1–mediated NIK cleavage occurred in the absence of Bcl10 (fig. S6F). Together, these findings suggest that NIK is a substrate for the MALT1 protease domain, but only when this domain is present within the context of API2-MALT1.

Structural analyses predict that the MALT1 protease should show specificity for substrates with a basic or uncharged residue at P1 (N-terminal to the cleavage site) (*19*). Furthermore, the MALT1 cleavage sites of Bcl10 and A20 both contain a P2-serine preceding a P1-arginine (*14*, *15*, *20*). Thus, we identified candidate P2-Ser/P1-Arg MALT1 cleavage sites within NIK that would generate fragments of ~37 and 70 kD (fig. S7A), and we individually changed each candidate P1-Arg to Ala. The R366A and R368A NIK mutants were readily cleaved by API2-MALT1; however, the R325A mutant was resistant (Fig. 3A), which suggests that API2-MALT1–dependent cleavage of NIK occurs at R325 (fig. S7B). Expression of the resulting C-terminal NIK cleavage fragment, NIK(326–947), which retains the kinase domain, induced robust p100 processing (fig. S7C), p52 nuclear translocation (Fig. 3B), and noncanonical NF-κB target gene expression (fig. S7D). NIK(326–947) also induced nuclear translocation of the p65 NF-κB subunit, which indicated activation of the canonical NF-κB pathway

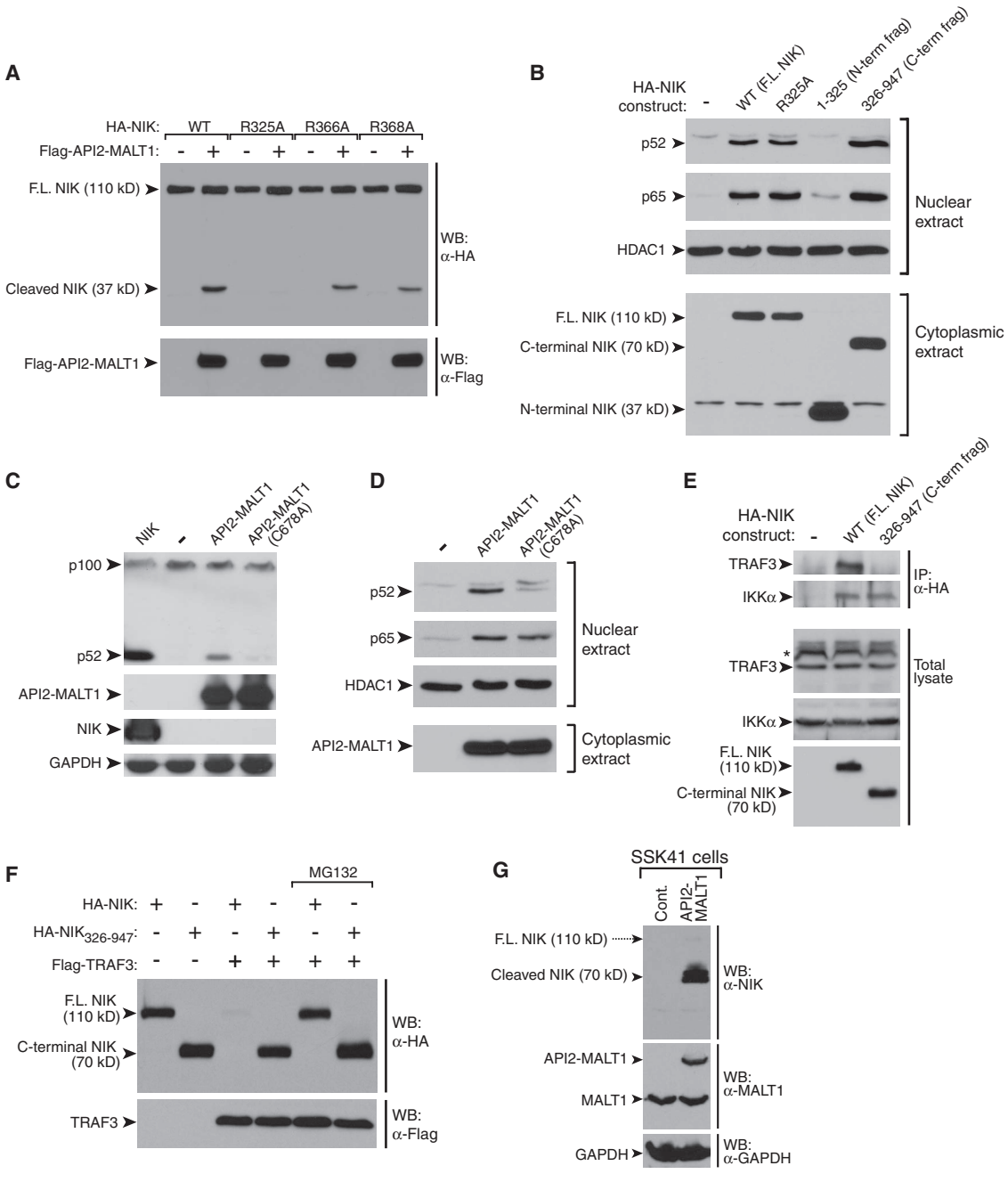

Fig. 3. API2-MALT1–dependent cleavage of NIK at R325 generates an active C-terminal fragment. (**A**) HEK293T cells were transfected as indicated, and the 37-kD N-terminal NIK cleavage fragment was detected by WB. (**B**) HEK293T cells were transfected as indicated, and nuclear translocation of p52 and p65 NF-κB subunits was assessed. (**C** and **D**) HEK293T cells were transfected as indicated, and endogenous p100 processing (C) and nuclear translocation of NF-κB subunits (D) were assessed. (**E**) HEK293T cells were transfected as indicated, and the ability of endogenous TRAF3 or IKKα to immunoprecipitate with each NIK protein was assessed. (**F**) HEK293T cells were transfected as indicated and then incubated in the absence or presence of 25 μM MG132. The presence of NIK was detected by WB. (**G**) Cell lysates were prepared in the absence of MG132 and analyzed by WB to detect full-length (F.L.) NIK and the 70-kD C-terminal NIK cleavage fragment. Data are representative of at least three separate experiments.

as well (Fig. 3B). Conversely, API2-MALT1-C678A, the catalytically inactive mutant that cannot induce NIK cleavage to produce NIK(326–947), failed to stimulate p100 processing (Fig. 3C) and p52 nuclear translocation (Fig. 3D and fig. S8). NIK associates with the adaptor protein, TRAF3, via an N-terminal NIK domain (amino acids 78 to 84), and this interaction targets NIK for proteasomal degradation (*21*–*23*). Because cleavage of NIK at R325 separates this TRAF3-binding site from the NIK kinase domain, we hypothesized that the active C-terminal NIK cleavage product would be resistant to TRAF3-directed degradation. Indeed, NIK(326–947) retained binding to IKKα but not to TRAF3 (Fig. 3E) and, unlike full-length NIK, was resistant to TRAF3-dependent proteasomal degradation (Fig. 3F). We also demonstrated the unique stability of the API2-MALT1–generated C-terminal NIK cleavage fragment in SSK41 B lymphoma cells. In the absence of MG132 (a proteosome inhibitor), expression of full-length NIK was very low, regardless of whether API2-MALT1 was present, consistent with the fact that NIK is subject to constitutive proteasomal degradation (*21*, *24*) (Fig. 3G). In contrast, high levels of endogenous C-terminal NIK cleavage fragment were detected in SSK41 cells expressing API2-MALT1 (Fig. 3G).

API2-MALT1–dependent generation of the C-terminal NIK cleavage fragment in SSK41 cells was associated with enhanced transcription of noncanonical NF-κB target genes, including *Pim-2*, an oncogenic kinase that blocks apoptosis by phosphorylating the proapoptotic Bcl-2 family member BAD (fig. S9, A and B) (*25*–*29*). RNA interference–mediated knockdown of NIK in API2-MALT1–expressing SSK41 cells led to loss of the 70-kD NIK fragment, loss of p100

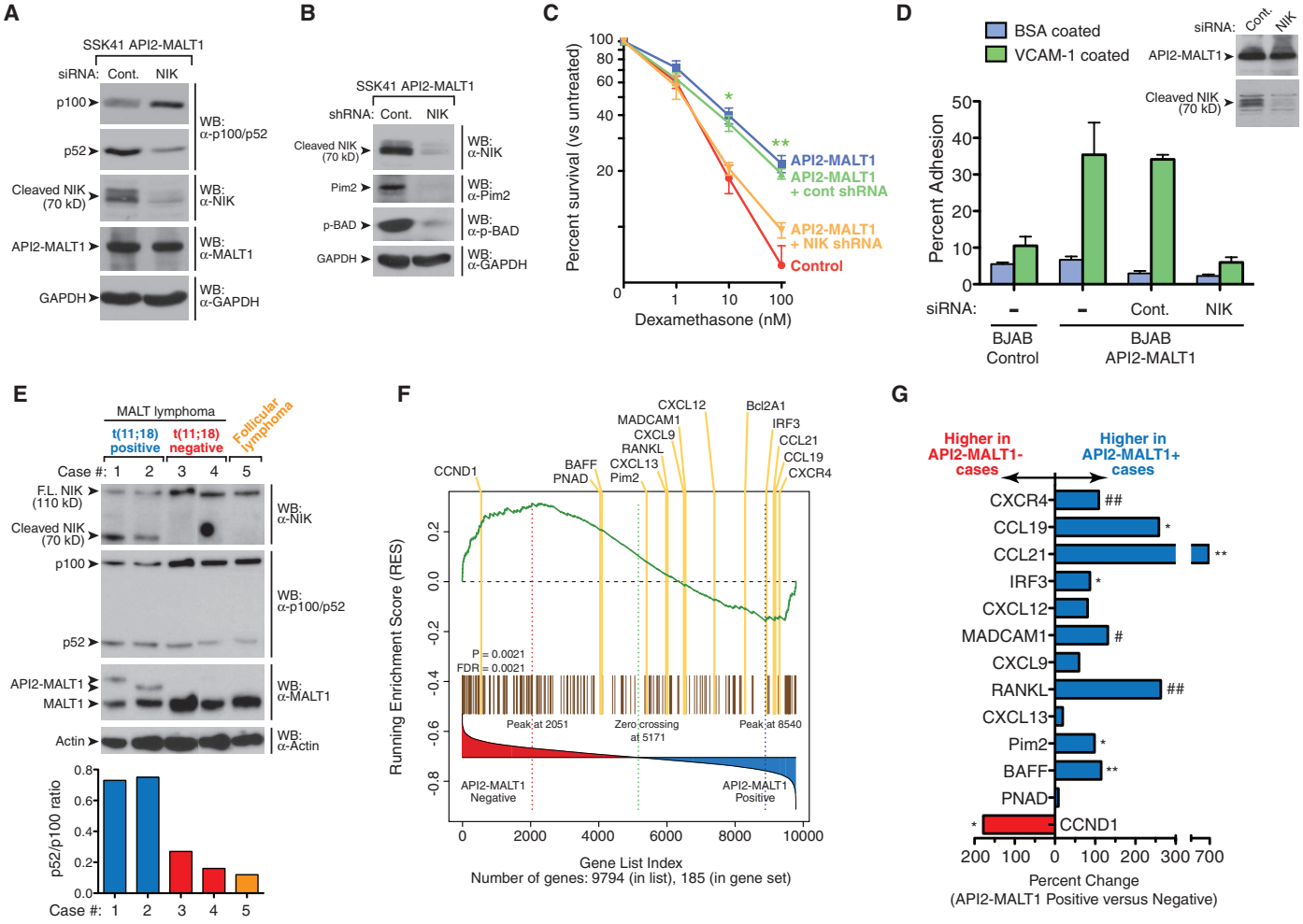

Fig. 4. API2-MALT1–dependent NIK cleavage is associated with up-regulation of noncanonical NF-κB target genes, results in an altered B cell phenotype, and occurs in t(11;18)-positive MALT lymphoma. (**A**) API2-MALT1–expressing SSK41 cells were transiently transfected with control or NIK small interfering RNA (siRNA), and p100 processing was assessed by WB. (**B** and **C**) API2-MALT1–expressing SSK41 cells were stably infected with control or NIK small hairpin RNA (shRNA) lentiviral particles. The 70-kD NIK cleavage fragment, Pim-2, and phospho-Ser^{112}–BAD levels were compared by WB (B). Cells were treated for 48 hours with dexamethasone, and percent viability was compared (C). Data are expressed as average ±SEM for four separate experiments. *$P < 0.005$, ** $P < 0.0001$. (**D**) API2-MALT1–expressing BJAB cells were transfected with control or NIK siRNA, and adhesion to VCAM-1–coated plates was assessed. Error bars represent SEM of duplicate determinations. Data are representative of three separate experiments. (**E**) Expression of API2-MALT1 in two t(11;18)-positive MALT lymphoma samples was confirmed by WB. p52/p100 ratios were quantified using densitometry. Both t(11;18)-positive cases had the same breakpoint in the *API2* gene (between exons 7 and 8) but different breakpoints in the *MALT1* gene [between exons 4 and 5 (case 1) and exons 6 and 7 (case 2)]. A follicular lymphoma and two t(11;18)-negative MALT lymphoma tumor specimens were used as controls. (**F**) GSEA of NF-κB target genes was performed in a set of MALT lymphomas with t(11;18) versus those without translocation from tumor collection no. 1 (*34*). The distribution of the genes is listed according to rank position, and known noncanonical NF-κB gene targets are highlighted in yellow. Absolute enrichment gave $P = 0.0021$ and false discovery rate (FDR) = 0.0021. (**G**) Comparison of noncanonical target gene expression in t(11;18)-positive versus negative cases from tumor collection no. 2 (*34*). Statistical testing for genes differentially expressed between the two types of MALT lymphomas was done by *t* test. $^{\#}P < 0.05$, $^{\#\#}P < 0.01$, $^{*}P < 0.005$, $^{**}P < 0.001$.

processing, and loss of API2-MALT1–dependent induction of Pim-2 kinase and BAD phosphorylation (Fig. 4, A and B). In accordance with its effect on antiapoptotic signal transduction, API2-MALT1 expression protected SSK41 cells from dexamethasone-induced cell death, which was reversed by NIK knockdown (Fig. 4, B and C, and fig. S10). Knockdown of IKKα impaired API2-MALT1–dependent protection, which supports a role for the noncanonical NF-κB pathway in mediating this effect of API2-MALT1–induced NIK cleavage (fig. S11). IKKβ knockdown impaired API2-MALT1–dependent protection as well, which implies that the canonical pathway may also contribute (fig. S11).

We next investigated the impact of API2-MALT1–dependent NIK cleavage on B cell adhesion because we had observed that API2-MALT1 induced the expression of B cell integrins (fig. S9A), known noncanonical NF-κB gene targets (*27*, *28*). API2-MALT1 expression was associated with increased B cell adhesion to plates coated with the endothelial protein vascular cell adhesion molecule VCAM-1, and this proadhesive phenotype was fully dependent on NIK (Fig. 4D). Lymphocyte adhesion is thought to play a role in lymphoma dissemination, thus NIK-cleavage–dependent API2-MALT1–induced adhesion may contribute to the higher rate of tumor spread among t(11;18)-positive MALT lymphomas (*1*). Again, knockdown of IKKα or IKKβ impaired API2-MALT1–dependent adhesion, which suggests that both noncanonical and canonical pathways contribute to the proadhesive phenotype after API2-MALT1–dependent NIK cleavage (fig. S12).

The striking pattern of NIK cleavage and stability observed in API2-MALT1–expressing B lymphoma cell lines was recapitulated in MALT lymphoma patient specimens. Full-length NIK levels were relatively low in all lymphomas, whereas an endogenous 70-kD C-terminal NIK fragment was detected only in t(11;18)-positive MALT lymphomas expressing API2-MALT1 (Fig. 4E). The presence of the NIK cleavage product was associated with an elevated p52/p100 ratio in the t(11;18)-positive tumors, which indicated enhanced noncanonical NF-κB activation (Fig. 4E). We performed absolute gene set enrichment analysis (GSEA) comparing the expression of NF-κB target genes between t(11;18)-positive MALT lymphomas (n = 9) and those with no translocation (n = 8). Analysis revealed a significant difference in the pattern of expression, with most known noncanonical NF-κB target genes overrepresented in the t(11;18)-positive cases (Fig. 4F, fig. S13, and tables S1 and S2). One exception is *cyclin D1,* although its categorization as a noncanonical NF-κB target gene is controversial (*30*). We then compared the expression of these noncanonical target genes in a completely separate group of six t(11;18)-positive and eight t(11;18)-negative MALT lymphomas that were collected at a different institution and, again, found that many noncanonical NF-κB target genes were more highly expressed in the t(11;18)-positive tumors (Fig. 4G). *CXCR4,* which encodes a chemokine receptor whose expression is associated with widespread lymph node involvement in B lymphomas (*31*–*33*), is one intriguing example of a noncanonical gene target that is up-regulated in t(11;18)-positive tumors in both tumor collections (Fig. 4, F and G) (*34*).

Deregulated NIK activity has been increasingly implicated in the pathogenesis of B cell neoplasms. For example, an EFTUD2-NIK fusion oncoprotein that retains the NIK kinase domain—but lacks the TRAF3-binding site and is resistant to proteasomal degradation—was recently identified in a case of multiple myeloma (*24*). Another recent report described a murine model of B lymphoproliferative disease in which a NIK mutant lacking the TRAF3-binding domain (NIKΔT3) was expressed in B cells (*35*). Compared with control transgenic mice expressing full-length NIK, the NIKΔT3 mice demonstrated increased NIK levels with enhanced p100 processing in B cells. They also showed expanded MALT and profound splenic marginal zone B cell hyperplasia, a phenotype that bears similarity to the Eμ-API2-MALT1 transgenic mouse (*36*). Together with our results, these findings suggest that separating the TRAF3-binding site on NIK from the kinase domain, either through aberrations of the *NIK* gene or through proteolytic cleavage of NIK protein, may represent a common mechanism for deregulating NIK activity in B cell neoplasms. Our findings suggest that in API2-MALT1–expressing MALT lymphomas, the API2 moiety mediates autooligomerization of API2-MALT1 and recruitment of NIK, and the MALT1 protease domain cleaves NIK, which leads to degradation-resistant NIK kinase and deregulated noncanonical NF-κB signaling (see model, fig. S14). Data suggest that NIK cleavage protects API2-MALT1–expressing B cells from apoptosis and promotes B cell adhesion, both of which could contribute to the more aggressive phenotype of t(11;18)-positive MALT lymphomas (*1*). Disrupting the API2-NIK interaction and/or blocking MALT1 protease or NIK kinase activity could represent new treatment approaches for refractory t(11;18)-positive MALT lymphoma.

References and Notes

1. P. G. Isaacson, M. Q. Du, *Nat. Rev. Cancer* **4**, 644 (2004).
2. M. Thome, *Nat. Rev. Immunol.* **8**, 495 (2008).
3. P. C. Lucas *et al.*, *J. Biol. Chem.* **276**, 19012 (2001).
4. L. Sun, L. Deng, C. K. Ea, Z. P. Xia, Z. J. Chen, *Mol. Cell* **14**, 289 (2004).
5. P. C. Lucas *et al.*, *Oncogene* **26**, 5643 (2007).
6. H. Zhou, M. Q. Du, V. M. Dixit, *Cancer Cell* **7**, 425 (2005).
7. Materials and methods are available as supporting material on *Science* Online.
8. T. D. Gilmore, *Oncogene* **25**, 6680 (2006).
9. N. L. Malinin, M. P. Boldin, A. V. Kovalenko, D. Wallach, *Nature* **385**, 540 (1997).
10. H. Y. Song, C. H. Régnier, C. J. Kirschning, D. V. Goeddel, M. Rothe, *Proc. Natl. Acad. Sci. U.S.A.* **94**, 9792 (1997).
11. S. L. Petersen *et al.*, *Cancer Cell* **12**, 445 (2007).
12. E. Varfolomeev *et al.*, *Cell* **131**, 669 (2007).
13. J. E. Vince *et al.*, *Cell* **131**, 682 (2007).
14. B. Coornaert *et al.*, *Nat. Immunol.* **9**, 263 (2008).
15. F. Rebeaud *et al.*, *Nat. Immunol.* **9**, 272 (2008).
16. Single-letter abbreviations for the amino acid residues are as follows: A, Ala; C, Cys; D, Asp; E, Glu; F, Phe; G, Gly; H, His; I, Ile; K, Lys; L, Leu; M, Met; N, Asn; P, Pro; Q, Gln; R, Arg; S, Ser; T, Thr; V, Val; W, Trp; and Y, Tyr.
17. H. Noels *et al.*, *J. Biol. Chem.* **282**, 10180 (2007).
18. D. Sanchez-Izquierdo *et al.*, *Blood* **101**, 4539 (2003).
19. A. G. Uren *et al.*, *Mol. Cell* **6**, 961 (2000).
20. L. M. McAllister-Lucas, P. C. Lucas, *Nat. Immunol.* **9**, 231 (2008).
21. G. Liao, M. Zhang, E. W. Harhaj, S.-C. Sun, *J. Biol. Chem.* **279**, 26243 (2004).
22. S. Vallabhapurapu *et al.*, *Nat. Immunol.* **9**, 1364 (2008).
23. B. J. Zarnegar *et al.*, *Nat. Immunol.* **9**, 1371 (2008).
24. C. M. Annunziata *et al.*, *Cancer Cell* **12**, 115 (2007).
25. G. Bonizzi *et al.*, *EMBO J.* **23**, 4202 (2004).
26. J. L. Chen, A. Limnander, P. B. Rothman, *Blood* **111**, 1677 (2008).
27. T. Enzler *et al.*, *Immunity* **25**, 403 (2006).
28. F. Guo, D. Weih, E. Meier, F. Weih, *Blood* **110**, 2381 (2007).
29. R. T. Woodland *et al.*, *Blood* **111**, 750 (2008).
30. I. I. Witzel, L. F. Koh, N. D. Perkins, *Biochem. Soc. Trans.* **38**, 217 (2010).
31. S. López-Giral *et al.*, *J. Leukoc. Biol.* **76**, 462 (2004).
32. Y. Nie *et al.*, *J. Exp. Med.* **200**, 1145 (2004).
33. M. Luftig *et al.*, *Proc. Natl. Acad. Sci. U.S.A.* **101**, 141 (2004).
34. See Materials and Methods in Supporting Online Materials for a description of the tumor collections nos. 1 and 2.
35. Y. Sasaki *et al.*, *Proc. Natl. Acad. Sci. U.S.A.* **105**, 10883 (2008).
36. M. Baens *et al.*, *Cancer Res.* **66**, 5270 (2006).

37. We thank M. Dyer for the SSK41 cells, R. Renne for the BJAB Tet-On cells, and G. Nunez for several expression plasmids. A Material Transfer Agreement is required for use of the SSK41 cells expressing API2-MALT1. Microarray data from MALT lymphoma tumor collections are Minimum Information About a Microarray Experiment (MIAME) compliant and are available online at the Gene Expression Omnibus (GEO) with accession number GSE25527 for collection no. 1 and accession number GSE25550 for collection no. 2 (www.ncbi.nlm.nih.gov/projects/geo/). L.M. is a recipient of the Nancy Newton Loeb Pediatric Cancer Research and Helen L. Kay Pediatric Cancer Research Awards and received support from National Institute of Child Health and Human Development, NIH, T32-HD07513. L.M. and S.R. were both supported by National Heart, Lung, and Blood Institute, NIH, T32-HL007622-21A2. M.B. is supported by grants from the Research Foundation—Flanders (FWO) and Belgian Foundation against Cancer. H.N. was an aspirant of the FWO-Vlaanderen. X.S. is a Senior Clinical Investigator of FWO-Vlaanderen, and P.V.L. is a postdoctoral researcher of the FWO. This work was supported by the Shirley K. Schlafer Foundation, the Elizabeth Caroline Crosby Fund, and grants from the University of Michigan Comprehensive Cancer Center (G007839), Leukemia and Lymphoma Research UK, and National Cancer Institute NIH (R01CA124540).

Supporting Online Material

www.sciencemag.org/cgi/content/full/331/6016/468/DC1
Materials and Methods
Figs. S1 to S14
Tables S1 and S2
References

12 October 2010; accepted 22 December 2010
10.1126/science.1198946